J Mater Sci (2009) 44:293–299
DOI 10.1007/s10853-008-3064-5

Ageing effects on α' precipitation and resistance to corrosion of a novel Cr–Mo stainless steel with high Mo content

Igor F. Vasconcelos · Sérgio S. M. Tavares · F. Evaristo U. Reis · Hamilton F. G. Abreu

Received: 23 January 2008 / Accepted: 15 October 2008 / Published online: 10 November 2008

Abstract The consequences of ageing at 400 and 475 °C on α' precipitation and corrosion resistance of a novel Cr–Mo ferritic SS with high Mo content were investigated. Combination of X-ray diffraction and Mössbauer spectroscopy results indicates the appearance of a small amount of a paramagnetic phase as a result of the ageing. This phase is iso-structural with the α phase and is thus associated with a Cr-rich α' phase. The appearance of this phase is related to a decrease of the resistance to corrosion as studied by DL-EPR because the presence of this paramagnetic phase leads to discontinuities in the oxide layer thus reducing corrosion protection and exposing the steel to the action of the corrosive solution.

Introduction

Corrosion in crude heavy oil processing has become a major problem in the oil industry. The current oil plants have been designed and constructed to process oil with low levels of naphthenic acidity. Discovery of heavy oil reservoirs has transformed the processing of highly acid oil into a major economic endeavor. The presence of naphthenic acids and sulfur complexes increases considerably the corrosion of parts subject to very high temperatures during oil processing.

The lining of distillation towers is probably the most affected part as it works under high temperature and pressure. According to reports from oil refineries, Mo-bearing stainless steels such as AISI 316L and AISI 317L are the preferred and the most effective lining materials. It is reported in the literature that addition of Mo in the alloy increases considerably its resistance to naphthenic acid corrosion [1, 2].

The use of austenitic stainless steels in linings has caused problems of cracking due to different thermal expansion coefficients of the lining and the base material, commonly a low alloy ferritic steel. An alternative would be a ferritic stainless steel with addition of Mo. In a previous work [3], we reported a study on the effects of low-temperature ageing on a AISI 444 steel that contains about 17.6% of Cr and 1.9% of Mo.

Ferritic stainless steels (SSs) are used in many manufacturing processes, mainly in the petrochemical industries. Ferritic steels are cheaper, have the same corrosion resistance of some austenitic grades (e.g., 304 SS or 316 SS), and present lower susceptibility to stress corrosion cracking (SCC). However, ferritic SSs are susceptible to some embrittlement phenomena such as grain growth, σ phase formation [4, 5], and α' precipitation [5, 6].

The precipitation of α' occurs at between 350 and 550 °C in ferritic and duplex SSs [5–7]. According to Grobner [6], α' formation in ferritic SSs with <17% Cr occurs by nucleation and growth, while above this level it occurs by spinoidal decomposition, as in, for example, duplex SSs.

It is well known that the presence of Cr and Mo in the alloy increases considerably its resistance to corrosion [1, 2]. On the down side, the increasing amounts of Mo

I. F. Vasconcelos (✉) · F. E. U. Reis · H. F. G. Abreu
Dep. Eng. Metalúrgica e de Materiais, Universidade Federal do Ceará, Campus do Pici Bloco 714, 60455-760 Fortaleza, CE, Brazil
e-mail: ifvasco@ufc.br

S. S. M. Tavares
Dep. Eng. Mecânica, Universidade Federal Fluminense, Niteroi, Brazil

make the alloy improper for machine work. This can, however, be circumvented by decreasing the Cr content. Moreover, the susceptibility of the ferritic steels to the α' precipitation increases with Cr but not considerably with Mo content. Therefore, a careful Cr–Mo content balance is needed in order to produce a corrosion-resistant alloy that is, at the same time, free of major α' precipitation.

In the present work, we investigate ageing effects on a novel Cr–Mo steel (with amounts of Mo higher than those found in commercial alloys) and its resistance to corrosion in the context of the formation of Cr-rich α' phase. This study is motivated by the possible substitution of AISI 316L and 317L SS in the distillation towers of petroleum-refining plants by Mo-rich, corrosion-resistant stainless steels.

Experimental procedure

Table 1 shows the chemical composition of the three alloys studied. Figure 1 shows the optical microscopy surface images of the as-received alloys showing a matrix 100% ferritic (gray phase). The as-received samples were solution-treated at 950 °C for 1 h and water-quenched. These were labeled A0, B0, and C0. The solution-treated samples were aged at 400 and 475 °C for times between 1 and 1000 h. The samples aged at 400 °C for 1, 10, 100, 500, and 1000 h were labeled A1 to A5, B1 to B5, and C1 to C5 while the ones aged at 475 °C were labeled AA1 to AA5, BB1 to BB5, and CC1 to CC5. These temperatures were selected because 400 °C is the maximum operational temperature in the distillation tower, while 475 °C is reported to be the temperature at which the kinetics of α' precipitation reaches a maximum [6].

Samples with a thickness of 0.04–0.06 mm were characterized at room temperature by transmission Mössbauer spectroscopy with a ^{57}Co source in Rh matrix and X-ray diffraction (XRD). Mössbauer velocity and isomer shift are relative to α-Fe. The Mössbauer spectra were fitted using Gaussian-shaped magnetic hyperfine field distributions and discrete subspectra. X-ray diffraction was performed in Bragg-Brentano geometry with CoKα source and a 0.02° 2θ step was chosen for all experiments.

The corrosion resistance was evaluated using double-loop electrochemical potentiodynamic reactivation (DL-EPR) tests. This is a practical and simple test, which was developed to detect and quantify sensitization in austenitic SSs [8]. Some authors have used this test to study the corrosion

Table 1 Chemical composition (in weight) of the F–Cr–Mo alloys and of the AISI 444 SS for comparison

Series	%Cr	%Mo	%C	%Cr-equivalent
A	18.3	7.7	<0.03	28.8
B	14.7	6.6	<0.03	23.7
C	13.0	6.2	<0.03	21.5
AISI 444	17.5	1.8	<0.03	19.4

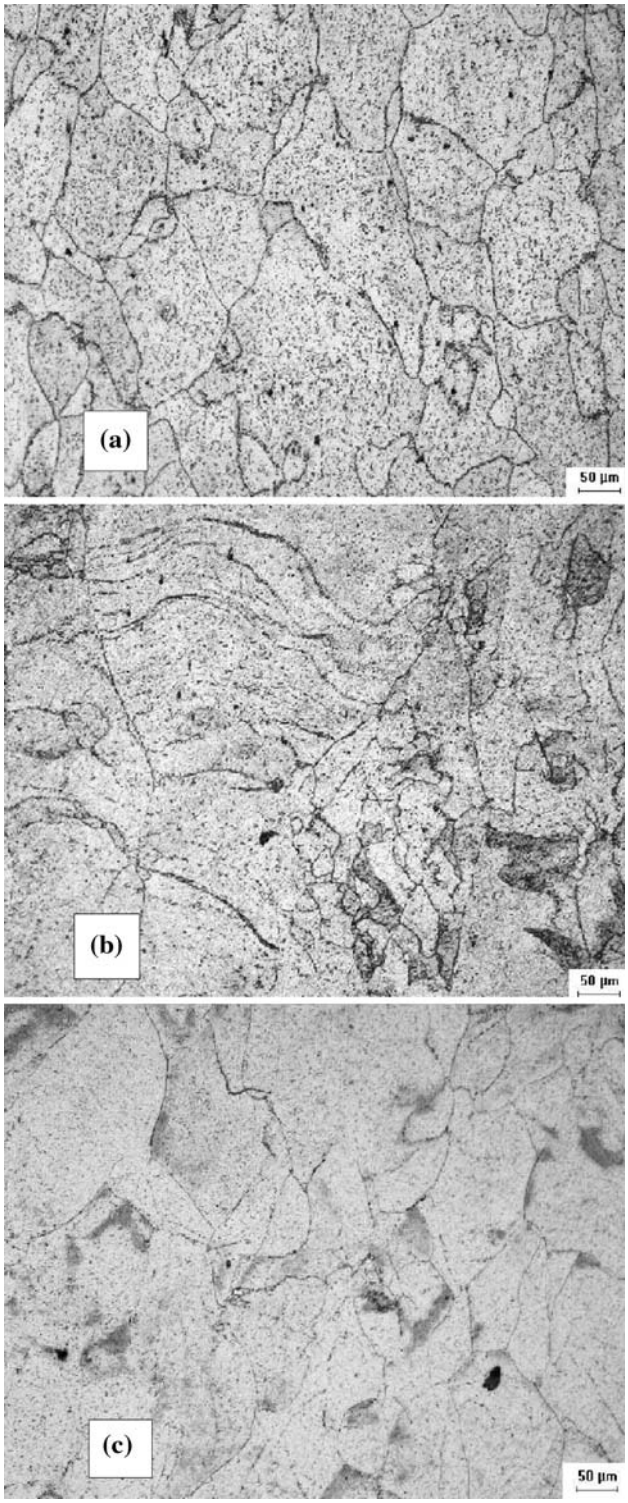

Fig. 1 Optical microscopy surface images of the as-received alloys: **a** A0, 18% Cr and 7.7% Mo; **b** B0, 15% Cr and 6.6% Mo; and **c** C0, 13% Cr and 6.2% Mo. The samples were etched with a hot 10% HNO_3 + 0.05% HF solution

resistance of duplex SSs aged at high [9] and low [10] temperatures. In this work, the DL-EPR tests were conducted using a conventional three-electrode cell with Pt foil as the auxiliary electrode and a saturated calomel electrode (SCE) as the reference electrode. The working electrode was constructed using steel samples embedded in epoxy resin. The experiments were initiated after a nearly steady-state open-circuit potential (E_{oc}) had been achieved (after ~30 min), followed by the potential sweep in the anodic direction at 1 mV/s until a potential of 0.3 V (versus SCE) was reached. Then, the scan was reversed in the cathodic direction until the E_{oc} was reached. Prior to each experiment, the working electrodes were polished on a 400-grit abrasive emery paper. The samples were then degreased with alcohol and cleaned in distilled water. The working solution was 0.5 M H_2SO_4 + 0.01 M KSCN (potassium thiocyanate). The localized corrosion susceptibility was evaluated from the ratio of I_r to I_a, where I_a is the peak current of the anodic scan and I_r is the peak current in the reverse direction [8]. All the measurements were performed at room temperature.

Results and discussion

Figure 2 shows X-ray diffraction patterns (a) and Mössbauer data (b) of the solution-treated samples. While the solution treatment temperature of 950 °C was sufficient to dissolve all allowing elements in the low Cr-equivalent samples B0 and C0, a small amount of an undissolved phase still remained in sample A0. This phase is indicated by the presence of a small peak in the XRD pattern (see arrow). The Mössbauer spectra of these samples (Fig. 2b-left panel) show a distribution of hyperfine magnetic field (BHF) (wide sextet) associated with the bulk α phase. The presence of a small amount of an undissolved phase in sample A0 is confirmed by the appearance of a second contribution (central singlet) to the Mössbauer spectrum. A singlet indicates this is a paramagnetic phase. A phase diagram for the composition of samples A0 was simulated using ThermoCalc® and is shown in Fig. 3. The vertical line at the solution treatment temperature of 950 °C suggests the undissolved phase is a Mo-rich χ phase. It should also be pointed out that the presence of alloying elements such as Cr and Mo in the vicinity of Fe atoms in the α matrix contributes to the decrease of BHF values from the value of 33 T expected for pure α-Fe. This explains the shift in the BHF distribution center toward higher values as the amount of allowing elements decreases (Fig. 2b-right panel).

The Mo-rich χ phase present in the solution-treated A0 samples remains undissolved after ageing times up to 1000 h at 475 °C, as can seen in Fig. 4a. Moreover, precipitation of Mo-rich χ phase does not increase as the ratio between the heights of the peak indicated by the arrow and

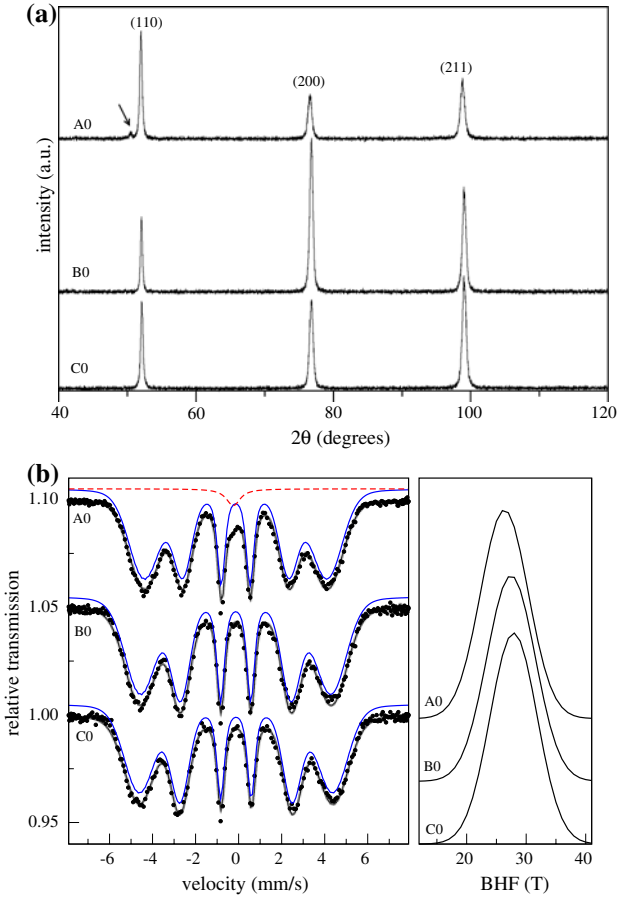

Fig. 2 XRD patterns (**a**) and Mössbauer spectra (**b**) for the samples after solution treatment. While the samples B0 (15% Cr) and C0 (13% Cr) are single phased (α phase; bcc ferrite), the sample A0 (18% Cr) presents a small amount of the Mo-rich χ phase (indicated by the arrow on the XRD pattern and the singlet on the Mössbauer spectrum)

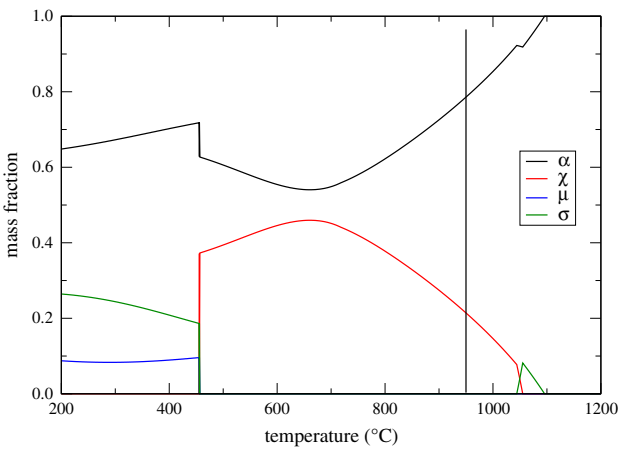

Fig. 3 ThermoCalc®-simulated phase diagram for the solution-treated sample A0 (18% Cr and 7.7% Mo). The vertical line at the temperature of solution treatment (950 °C) suggests the presence of some amount of χ phase for this composition

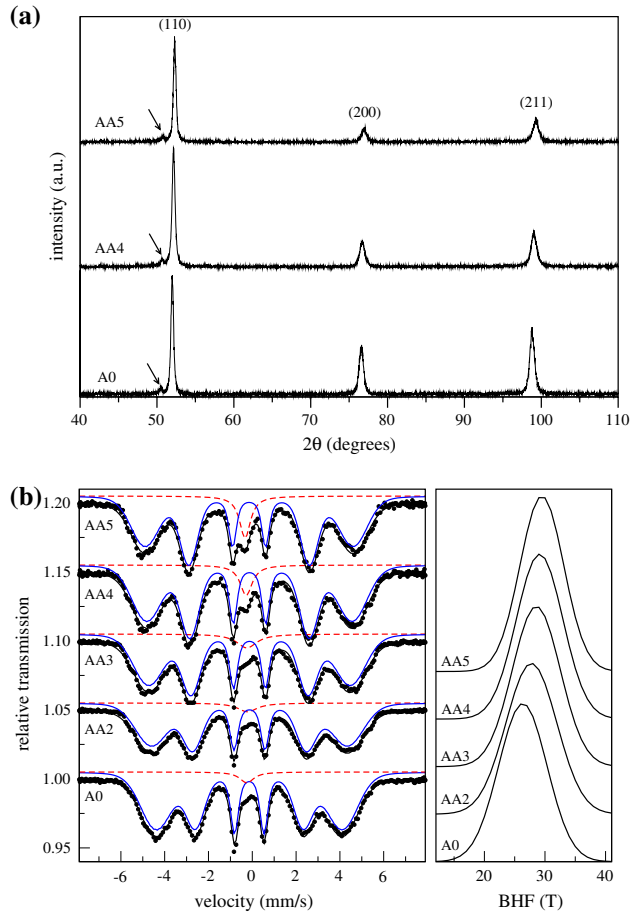

Fig. 4 XRD patterns (**a**) and Mössbauer spectra (**b**) for the AA samples (18% Cr, 7.7% Mo; aged at 475 °C)

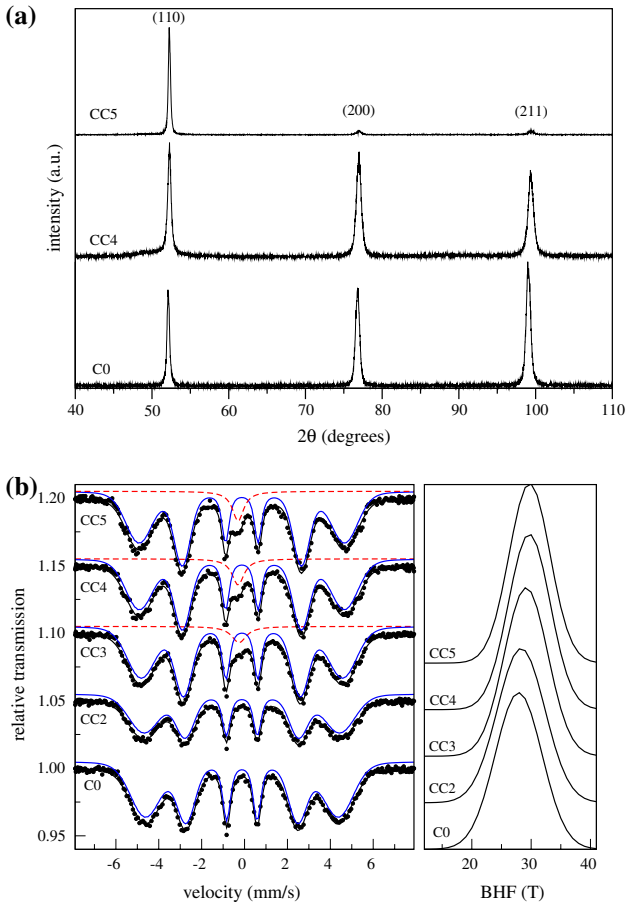

Fig. 5 XRD patterns (**a**) and Mössbauer spectra (**b**) for the CC samples (13% Cr, 6.2% Mo; aged at 475 °C)

the main α phase peak stays unchanged. However, the increase in the area of the singlet in the Mössbauer spectra for ageing times of 100 h and up (Fig. 4b-left) indicates the precipitation of another paramagnetic phase. This phase is iso-structural with the α phase as no extra peaks appear in the XRD patterns and is thus associated with a Cr-rich α′ phase. BHF distributions in Fig. 4b-right shows a shift in the average field distribution toward higher values. This is consistent with the reduction of the Cr content in the α phase matrix due to the precipitation of Cr-rich α′.

As for the A series, the lower Cr-equivalent C series presents precipitation (for ageing times of 100 h and up at 475 °C) of a second phase indicated by the appearance of a singlet in the Mössbauer spectra in Fig. 5b-left. Again, the absence of extra peaks in the XRD patterns (Fig. 5a) indicates this phase is iso-structural with the α phase and is associated with a Cr-rich α′ phase. The XRD patterns and Mössbauer spectra of B series samples are very similar to the ones in Fig. 5 and are not shown. Likewise, ageing effects at 400 °C are similar to those at 475 °C and therefore are not shown as well. The evolution of the paramagnetic volume with ageing time for the A and C series is shown in Fig. 6.

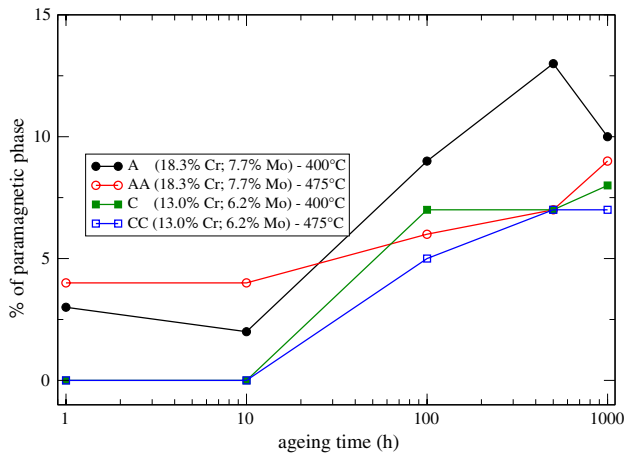

Fig. 6 Amount of paramagnetic phase as a function of ageing time at 400 and 475 °C. Obtained from the Mössbauer spectra as the ratio between the areas under the singlet and the entire spectrum

Precipitation of α′ phase is the most likely candidate to explain the appearance and increase of paramagnetic singlet in ferritic and duplex stainless steels aged at 400 and 475 °C. The high Cr and Mo contents of this phase change

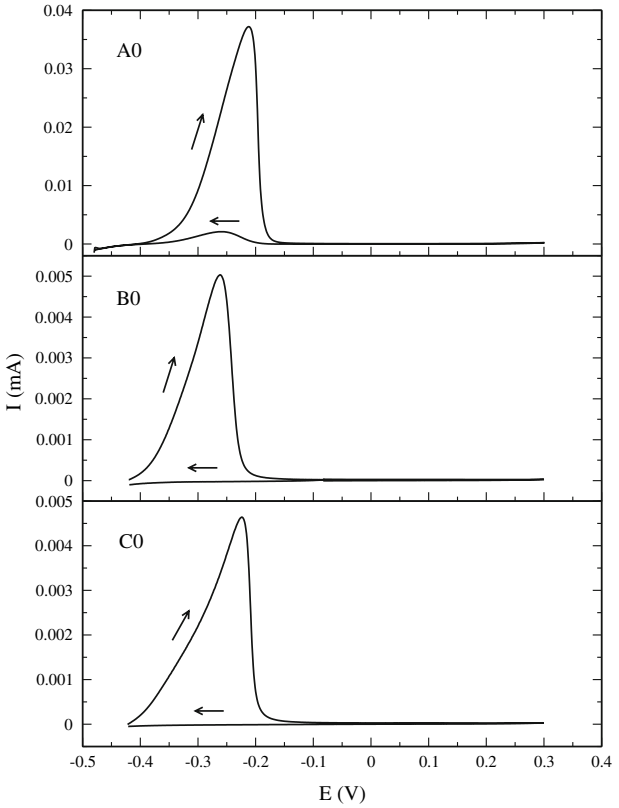

Fig. 7 DL-EPR curves for the solution-treated samples

its magnetic behavior from ferro- to paramagnetic. This effect was observed and explained by Solomon and Levinson in high Cr alloys [7]. The occurrence of α' precipitates in the low Cr content steels studied in this work is probably due to the enhancing effect of Mo in the kinetics of α' precipitation.

Figure 7 shows the DL-EPR curves of samples A0, B0, and C0. The main result of the DL-EPR test is the I_r/I_a ratio. The presence of a reactivation peak indicates that the material has Cr-depleted microregions. The higher the reactivation current (I_r), the lower the corrosion resistance. Steels B and C do not present reactivation peaks in the solution-treated condition, while sample A0 presents a small one, certainly due to the Mo-rich χ phase.

The DL-EPR curves of samples A5, C5, AA5, and CC5 are shown in Fig. 8. Pronounced reactivation peaks are observed due to the precipitation of Cr-rich α' phase, which creates Cr-depleted zones in the matrix. The process is similar to sensitization due to chromium carbide precipitation in austenitic stainless steels, but it is not concentrated in the grain boundaries and it is much finer and more dispersed. Figure 9 shows the surface images of the samples C0 and C5 after the DL-EPR tests. While the unaged sample was not attacked during the test (Fig. 9a), the sample aged at 400 °C for 1000 h shows a highly attacked surface, with many submicropits (Fig. 9b).

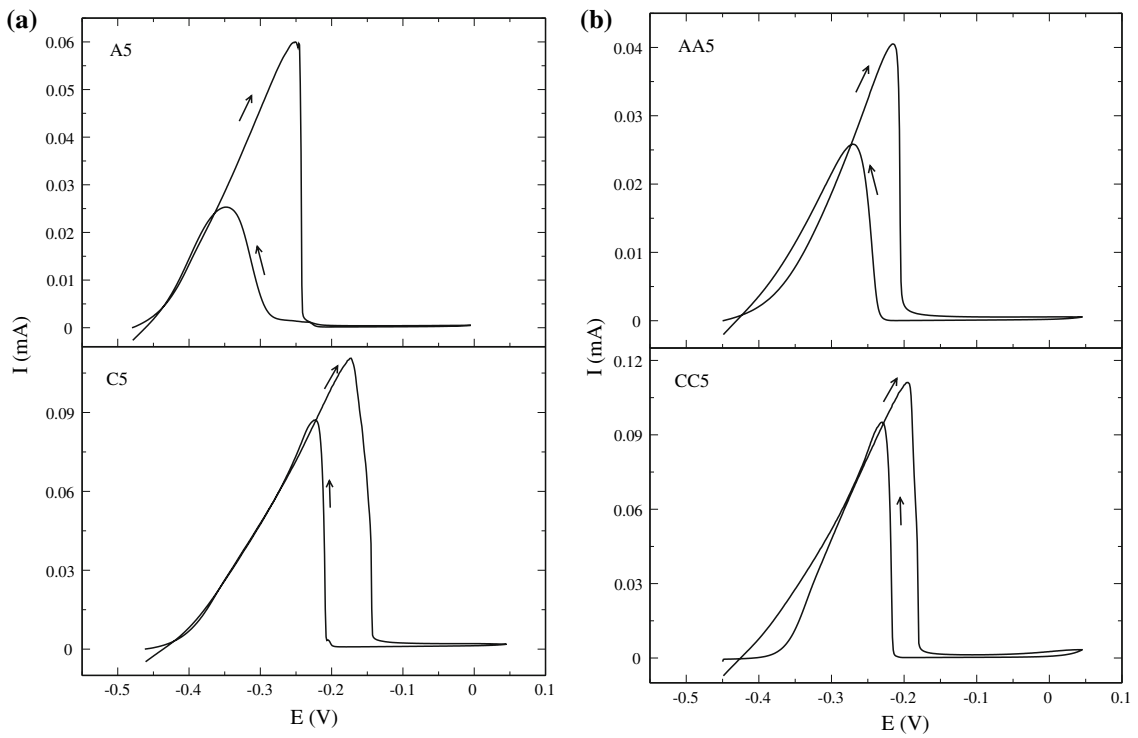

Fig. 8 DL-EPR curves for samples aged for 1000 h at **a** 400 °C and **b** 475 °C

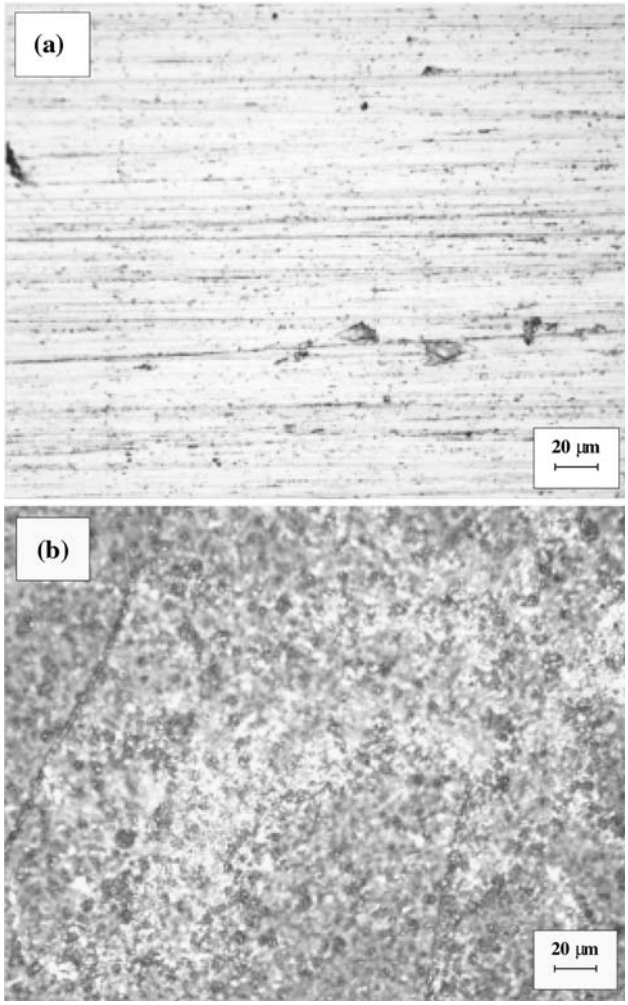

Fig. 9 Optical microscopy of sample C used in the DL-EPR tests: **a** unaged and **b** after ageing for 1000 h at 400 °C (500×)

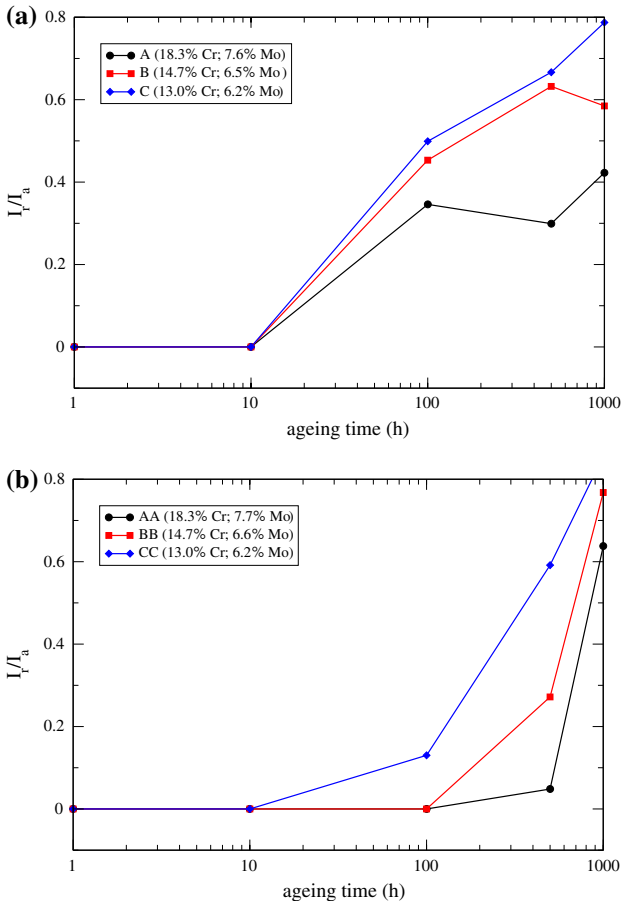

Fig. 10 The ratio of I_r to I_a as a function of ageing time at **a** 400 °C and **b** 475 °C

Figure 10 shows the behavior of the I_r/I_a ratio as a function of the ageing time at 400 and 475 °C, respectively, for the three compositions investigated. It can be inferred from the analysis of these curves that, in the presented ageing conditions, increase in Cr content leads to decrease of the I_r/I_a ratio, as the Mo content is similar in all samples. Also, the increase of I_r/I_a occurs more rapidly in samples aged at 400 °C than at 475 °C. Previous work [3, 5, 7, 11] on the low-temperature ageing of ferritic and duplex stainless steel has shown that the ageing effects are more pronounced at 475 °C. Based on the DL-EPR results presented, however, it seems that in these high Mo alloys the more critical ageing temperature is 400 °C.

The rise of the I_r/I_a ratio with ageing time shown in Fig. 10 is associated with the increase of the paramagnetic phase volume obtained by Mössbauer spectroscopy, shown in Fig. 6. The presence of this paramagnetic phase leads to discontinuities in the oxide layer thus reducing corrosion protection and exposing the steel to the action of the corrosive solution.

Conclusions

The effects of ageing at 400 and 475 °C on a novel Cr–Mo (with high amounts of Mo) ferritic stainless steel were investigated. Three alloys with different Cr-equivalent contents were solution-treated at 950 °C for 1 h and quenched in water. X-ray diffraction and Mössbauer spectroscopy measurements reveal a small amount of an undissolved paramagnetic phase in the sample with the higher Cr-equivalent content while the other two samples were completely dissolved. A ThermoCalc® simulation suggests this phase is a Mo-rich χ phase and DL-EPR curves indicate a reduction to corrosion resistance due to its presence.

X-ray diffractograms do not suggest any changes in the structure of the samples as a consequence of ageing at 400 and 475 °C. Mössbauer spectra, on the other hand, show the appearance (or increase, in the sample with the highest

Cr-equivalent content) of a paramagnetic phase induced by the ageing process, due to the formation of a fine Cr-rich α' phase. Pronounced reactivation peaks in the DL-EPR curves are observed due to the precipitation of this Cr-rich α' phase, which creates Cr-depleted zones in the matrix, thus decreasing the alloys' resistance to corrosion.

Mössbauer spectroscopy is a precise local technique that allows for identification of Fe-bearing phases that might not be readily identifiable by X-ray diffraction. These two techniques have been shown to be complementary and very useful in determining the phase content of the alloys studied, which is corroborated by DL-EPR results.

Acknowledgements The authors are grateful to the Brazilian research agencies Fundação Cearense de Apoio ao Desenvolvimento Científico e Tecnológico (FUNCAP); Conselho Nacional de Desenvolvimento Científico e Tecnológico (CNPq); and Agência Nacional de Petróleo (ANP) for financial support, and to Prof. Pedro de Lima Neto for DL-EPR measurements.

References

1. Zetlmeisl MJ (1996) Corrosion'96, paper no. 218
2. Wu XQ, Jing HM, Zheng YG, Yao ZM, Ke W (2004) Corros Sci 46:1013
3. Souza JA, Abreu HFG, Nascimento AM, de Paiva JAC, de Lima-Neto P, Tavares SSM (2005) J Mater Eng Perform 14:367
4. Kuzucu V, Aksoy M, Korkut MH, Yildirim MM (1997) Mater Sci Eng A 230:75
5. Van Zwieten ACTM, Bulloch JH (1993) Int J Press Vessels Piping 56:1
6. Grobner PJ (1973) Metall Trans 4:251
7. Solomon HD, Levinson LM (1978) Acta Metall 28:429
8. Sedricks AJ (1996) Corrosion of stainless steel, 2nd edn. Wiley-Interscience, New York
9. Lopez N, Cid M, Puigalli M, Azkarate I, Pelayo A (1997) Mater Sci Eng A 229:123
10. Park CJ, Kwon HS (2002) Corros Sci 44:2817
11. Tavares SSM, Terra VF, de Lima-Neto P, Matos DE (2005) J Mater Sci 40:4025. doi:10.1007/s10853-005-1993-9